ELSEVIER

Surface Science 454–456 (2000) 837–841

surface science

www.elsevier.nl/locate/susc

Self-assembled metal–semiconductor compound nanocrystals on Group IV semiconductor surfaces

I. Goldfarb *, G.A.D. Briggs

University of Oxford, Department of Materials, Parks Road, Oxford OX1 3PH, UK

Abstract

Nanocrystals of material B may form on a substrate of material A in order to relieve the strain from the B/A crystalline mismatch. In the most simplistic approximation, if such an elastic relaxation outweighs the additional surface energy due to the island walls, it will create the thermodynamic tendency for the nanocrystal formation. Hence one can 'engineer' ultra-small and crystallographically perfect nanocrystal self-assemblies by careful selection of a film/substrate system under appropriate growth conditions. In this work, intentional nanocrystal creation is demonstrated in semiconductor/semiconductor and metal/semiconductor systems, such as Ge/Si, Co/Si, and Co/Ge/Si. The growth of the nanocrystals was observed using in situ scanning tunnelling microscopy and reflection high energy electron diffraction. In spite of the marked differences in surface thermodynamics and kinetic pathways, the different material combinations lead to remarkably similar nanocrystal arrays on the surface.

Keywords: Epitaxy; Reflection high-energy electron diffraction (RHEED); Scanning tunneling microscopy; Self-assembly; Silicides; Silicon–germanium; Surface structure, morphology, roughness, and topography

1. Introduction

Since the discovery of strain-induced three-dimensional (3D) semiconductor islands [1–3], self-assembled nanocrystals have attracted much attention, originally in relation to quantum-dot devices. The major advantage of such dots is their nanometre size, which compares favourably with the inevitably larger dot sizes obtained by micro-lithography. However, the self-assembled arrays lack regularity and uniformity routinely obtained by lithographic patterning [4,5]. Therefore, much effort has been directed at achieving an adequate understanding of the factors governing self-assembled nanocrystal growth [6–13], and thus the size-uniformity and spatial and vertical positioning [14–18].

In the first instance a growth mode can be predicted on the basis of the layer/substrate lattice mismatch. At small enough mismatch layer-by-layer (Frank–van der Merwe) growth is expected, e.g. in fully matched homoepitaxy, while at larger mismatch 3D growth will commence either immediately (Volmer–Weber) or after few 2D monolayers (Stranski–Krastanow). Such expectations are based on the elastic strain relaxation by the island, in a coherent island/substrate system, where the island volume is inversely proportional to the sixth power of the mismatch [6,7]. However, the

* Corresponding author. Present address: Department of Solid Mechanics, Materials and Structures, The Iby and Aladar Fleischman Faculty of Engineering, Tel Aviv University, 69978 Ramat Aviv, Israel. Fax: +972 3 640 7617.

E-mail address: ilang@eng.tau.ac.il (I. Goldfarb)

0039-6028/00/$ - see front matter
PII: S0039-6028(00)00227-2

volume is also directly proportional to the third power of the surface and interface energy term [6,7], and also depends on the edge and corner energy terms [14]. Hence the lattice mismatch criterion alone should be applied with caution, only to compare between heterosystems with similar surface energies. For example, continuous reduction of nanocrystal size with increasing Ge content x, and thus increasing mismatch, in a $Si_{1-x}Ge_x$/Si system has been indeed experimentally observed [19]. In this system the surface and interface energy variations with increasing mismatch are small in comparison with the corresponding increase in the elastic strain energy. In contrast, larger nanocrystals due to smaller mismatch might have been expected in a $CoSi_2$/Si system, contrary to the experimental observations [20,21]. This can be explained if, for example, the surface and interface energy term in this system is also accordingly smaller. Unfortunately the latter quantity is rarely known.

Metal–semiconductor compounds, e.g. silicides, offer continuous variation of lattice mismatches with Si, ranging from 0.4% for $NiSi_2$, up to more than 10% for Group IV transition metals. Thus depending on the metal and stoichiometry of the compound, a combination of the lattice mismatch and surface and interface energy can drive the system towards surface roughening in the form of undulations or nanometre-size 3D islands [22–24]. In this work we show three different experimental systems, which all exhibit the formation of surface nanocrystals. The ability to introduce nano-roughness in a controlled fashion is useful not only for quantum-dot devices, but also for heterogeneous catalysis, gas sensing, and micro- and nano-electromechanical devices.

2. Experimental

Details of our sample preparation, growth, and STM acquisition are given in our previous work [25–29]. Briefly, chemically treated n-type Si(001) substrates were degassed in UHV, mounted in the STM stage (JEOL JSTM-4500XT), flashed at 1150°C, quenched to $T \leq 600$°C, and slowly cooled to the desired growth temperature (from room temperature to 500°C). The samples for Ge growth were then exposed to germane (GeH_4) in the 10^{-7}–10^{-5} Pa range and constant-current STM images (with currents around 0.1 nA and voltages in the ± 3 V range) were acquired in real time, during the exposure. To avoid metal-induced $(2 \times N)$ reconstruction, the samples were handled with ceramic tweezers and clamped to the Ta support on the holder by Ta clamps. Sample cleanness was routinely checked by Auger electron spectroscopy (AES), to yield contamination-free surface. During the sample flashes and anneals, the pressure was kept below 10^{-7} Pa. Such treatment has generally proved effective in producing well-ordered Si(2×1) surfaces.

To promote trench-nucleation for cobalt silicide growth, Ni-contaminated Si$(2 \times N)$ substrates were used [21]. A thin Ge/Si(001) layer, grown to a less than a Stranski–Krastanow critical thickness, and therefore two dimensional, was used as a substrate for cobalt germanide growth. Co was supplied from a water-cooled four-element e-beam evaporator at 45° to the sample, with the evaporation pressure not exceeding 10^{-7} Pa. Silicide and germanide growth was also monitored in real time with STM; however, owing to the shadowing of the metal flux by the tip, RHEED monitoring proved more effective.

12 kV RHEED patterns, with the electron beam parallel to Si⟨110⟩, were recorded from the screen (located 23 cm from the sample) and computer analysed using conventional image-processing software. Accuracy of the interatomic spacing measurements was ± 0.10 Å (corresponding to $\pm 2.60\%$ of the Si (001) surface lattice constant, $a = 3.84$ Å).

3. Results and discussion

To control the nanocrystal size, shape and location, one must learn about their nucleation. Although Ge/Si(001) nanocrystals nucleate heterogeneously at various surface irregularities, the nucleation does not take place at the Ge/Si(001)-$(M \times N)$ vacancy trenches [25–29]. Hence the only way to align Ge nanocrystals is at the step edges. The case is different when Co is deposited onto the trenched Si surface. Fig. 1 shows that immedi-

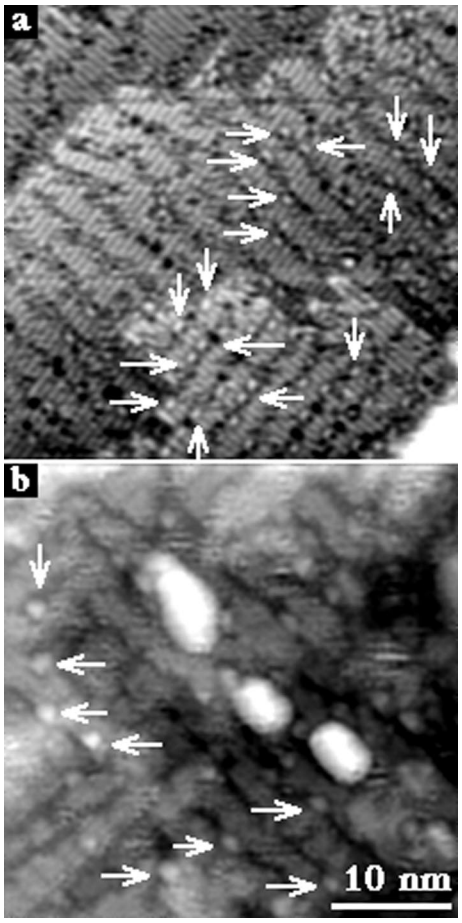

Fig. 1. Real-time STM observation of cobalt (a) silicide and (b) germanide nucleation at the trenches of the Ni-induced Si(001)-$(2\times N)$ surface, and Ge/Si(001)-$(M\times N)$ surface, respectively. White arrows point to some of the nuclei. Note also three grown nanocrystals in (b).

ately upon opening the evaporator shutter, tiny nuclei appear inside either Ni-induced Si(001)-$(2\times N)$ trenches (Fig. 1a), or Ge/Si(001)-$(M\times N)$ trenches (Fig. 1b). The experiments were partly aimed at evaluating the possibility of creating interconnects on the atomic scale, using these natural patterns of strain-induced line defects. In spite of the evidently successful silicide and germanide nucleation at the trenches, there was no alignment of the grown nanocrystals along the trenches. A possible reason for that failure can be inferred from Fig. 1b, where three grown germanide nanocrystals are shown alongside the nuclei. Their lateral dimensions are comparable with the periodicity of vacancy trenches, and the probable elastic repulsive interaction between the nanocrystals can prevent them from lining up along the trenches in close vicinity to one another. Hence it appears that different, perhaps more wetting, metals should be used to form that kind of trench-patterned interconnects.

Arrays of fully grown nanocrystals with their corresponding RHEED patterns are shown in Fig. 2. Figs. 1b and 2a show the Ge/Si(001)-$(M\times N)$ surface, typical of a wetting layer prior to Krastanow transition. This surface has been characterised by us in detail, both in STM [25–28] and RHEED [30], and will not be described here. The splitting of the full-order diffracted beams in the inset of Fig. 2a reflects the periodicity of the $(M\times N)$ trenches, unlike the case of Ni-induced trenches in Fig. 1a, which usually cause only unresolved line broadening [30]. When more Ge is deposited onto this $(M\times N)$ surface, Ge nanocrystals also known as 'hut clusters' nucleate, as shown in Fig. 2b. However, if Ge deposition is stopped at this point and Co is evaporated instead and annealed, cobalt germanide nanocrystals, such as those shown in Fig. 2d, are realised. Cobalt evaporation onto an Si(2×1) or Si$(2\times N)$ surface (as shown in Fig. 1a) results in cobalt disilicide nanocrystal arrays, shown in Fig. 2c.

The kinetics of Ge epitaxial growth is very different from that of a metal–semiconductor compound growth, as in the latter a chemical reaction takes place. Even between silicides and germanides the phase formation kinetics may differ considerably. Nonetheless the nanocrystal shape in all cases is rather similar, a four-facet prism, implying that the same elastic strain relaxation argument is responsible for this low energy shape [6,7]. As the lowest energy shape is a square-based pyramid, rather than a prism [6,7], the nanocrystals are apparently not in equilibrium, although can be brought closer to it [12,13,21]. Ge nanocrystals are almost perfectly shaped prisms with four {501} facets, elongated parallel to the Si⟨100⟩ directions, while the silicide and especially germanide nanocrystals are less well geometrically defined [21], and elongate parallel to the Si⟨110⟩ directions. Not only the shape, but also the crystalline

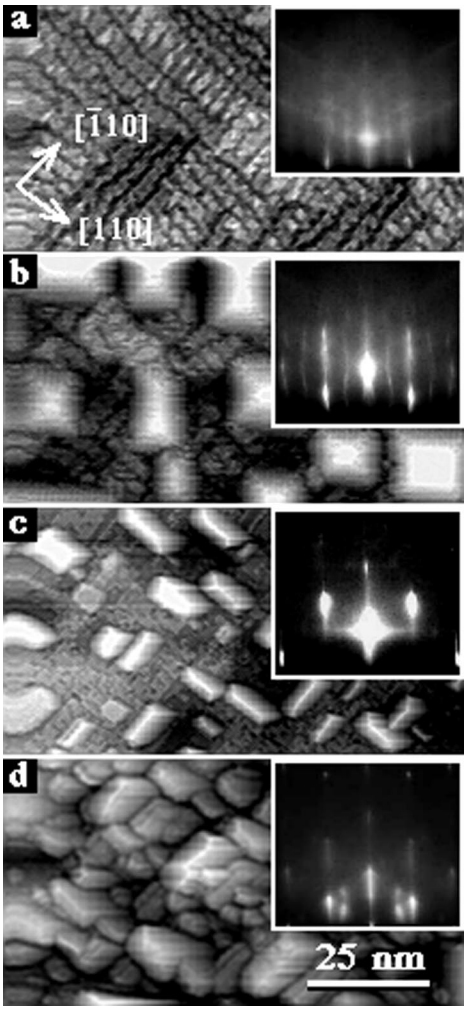

Fig. 2. (a) Ge/Si(001)-($M \times N$) surface prior to Stranski–Krastanow transition, and the corresponding RHEED pattern. (b) Ge/Si(001) 'hut' nanocrystals formed upon additional Ge deposition onto Ge/Si(001)-($M \times N$) shown in (a). Ge coverage is about 8 ML. Note the characteristic chevron-type RHEED pattern in the inset. (c) Cobalt silicide nanocrystals formed upon Co deposition onto Ni-induced Si(001)-($2 \times N$) surface, as shown in Fig. 1a, with their RHEED pattern. (d) Cobalt germanide nanocrystals formed upon Co deposition onto Ge/Si(001)-($M \times N$) surface, as shown in (a) and in Fig. 1b, with characteristic RHEED pattern. Both germanide and silicide coverage is in the submonolayer range. In all the RHEED patterns the electron beam was parallel to Si$\langle 110 \rangle$ directions.

structure and orientation relations differ when going from Fig. 2b to Fig. 2c and d, as indicated by distinct diffraction patterns in the respective insets. Ge {501}-faceted nanocrystals exhibit diamond structure and are oriented with their {001} planes parallel to the surface [2,6–13,25–28], and {111}- and {110}-faceted $CoSi_2$ nanocrystals have their {221} planes parallel to the surface [21]. The mean size and number densities differ as well, with the silicide nanocrystals being smaller than even the smallest possible Ge nanocrystals [21]. In contrast, as follows from comparing Fig. 2b with Fig. 2c, growth anisotropy is smaller for the Ge islands. Cobalt germanide nanocrystals are more closely packed, and their anisotropic elongation is smaller, more comparable with that of the Ge nanocrystals. The exact stoichiometry, and thus phase and structure, and the orientation relations of these germanide nanocrystals are yet to be determined.

4. Conclusions

One of the key parameters in determining the surface morphology in heteroepitaxy is the lattice mismatch between the substrate and the epilayer. When the mismatch is very small, the growth is layer by layer, and the resulting morphology is two dimensional. When the mismatch is too large, the strain is relaxed inelastically, by misfit dislocations. In this work we demonstrate how, by choosing intermediate mismatch values, Ge, silicide, and germanide nanocrystal arrays can be created on the growing surface in a controlled manner. Their different shape, size, and density distributions can be used for quantum-dot devices, to catalyse chemical reactions, to reduce adhesion between surfaces in microelectromechanical systems, etc. More quantitative predictions of surface evolution in heteroepitaxy require the knowledge of relevant surface, interface, and other energies.

References

[1] D.J. Eaglesham, M. Cerullo, Phys. Rev. Lett. 64 (1990) 1943.
[2] Y.-W. Mo, D.E. Savage, B.S. Swartzentruber, M.G. Lagally, Phys. Rev. Lett. 65 (1990) 1020.

[3] S. Guha, A. Madhukar, K.C. Rajkumar, Appl. Phys. Lett. 57 (1990) 2110.
[4] R. Nötzel, Semicond. Sci. Technol. 11 (1996) 1365.
[5] E.S. Kim, N. Usami, Y. Shiraki, Semicond. Sci. Technol. 14 (1999) 257.
[6] J. Tersoff, R.M. Tromp, Phys. Rev. Lett. 70 (1993) 2782.
[7] J. Tersoff, F.K. LeGoues, Phys. Rev. Lett. 72 (1993) 3570.
[8] D.E. Jesson, K.M. Chen, S.J. Pennycook, T. Thundat, R.J. Warmack, Phys. Rev. Lett. 77 (1996) 1330.
[9] D.E. Jesson, G. Chen, K.M. Chen, S.J. Pennycook, Phys. Rev. Lett. 80 (1998) 5156.
[10] M. Kästner, B. Voigtländer, Phys. Rev. Lett. 82 (1999) 2745.
[11] G. Medeiros-Ribeiro, A.M. Bratkowsky, T.I. Kamins, D.A.A. Ohlberg, R.S. Williams, Science 279 (1998) 353.
[12] G. Medeiros-Ribeiro, T.I. Kamins, D.A.A. Ohlberg, R.S. Williams, Phys. Rev. B 58 (1998) 3533.
[13] T.I. Kamins, G. Medeiros-Ribeiro, D.A.A. Ohlberg, R.S. Williams, J. Appl. Phys. 85 (1999) 1159.
[14] V.A. Shchukin, N.N. Ledentsov, P.S. Kop'ev, D. Bimberg, Phys. Rev. Lett. 75 (1995) 2968.
[15] F. Liu, M.G. Lagally, Surf. Sci. 386 (1997) 169.
[16] T. Ogino, Surf. Sci. 386 (1997) 137.
[17] J.-H. Zhu, K. Brunner, G. Abstreiter, Appl. Phys. Lett. 73 (1998) 620.
[18] J. Tersoff, C. Teichert, M.G. Lagally, Phys. Rev. Lett. 76 (1996) 1675.
[19] W. Dorsch, H.P. Strunk, H. Wavra, G. Wagner, J. Groenen, R. Carles, Appl. Phys. Lett. 72 (1998) 179.
[20] V. Scheuch, B. Voigtländer, H.P. Bonzel, Surf. Sci. 372 (1997) 71.
[21] I. Goldfarb, G.A.D. Briggs, Phys. Rev. B 60 (1999) 4800.
[22] C.W.T. Bulle-Lieuwma, A.H. Van Ommen, J. Hornstra, C.N.A. Aussems, J. Appl. Phys. 71 (1992) 2211.
[23] D.P. Adams, S.M. Yalisove, D.J. Eaglesham, J. Appl. Phys. 76 (1994) 5190.
[24] V. Buschmann, M. Rodewald, H. Fuess, G. Van Tendeloo, C. Schäffer, J. Cryst. Growth 191 (1998) 430.
[25] I. Goldfarb, P.T. Hayden, J.H.G. Owen, G.A.D. Briggs, Phys. Rev. Lett. 78 (1997) 3959.
[26] I. Goldfarb, P.T. Hayden, J.H.G. Owen, G.A.D. Briggs, Phys. Rev. B 56 (1997) 10 459.
[27] I. Goldfarb, J.H.G. Owen, P.T. Hayden, D.R. Bowler, K. Miki, G.A.D. Briggs, Surf. Sci. 394 (1997) 105.
[28] I. Goldfarb, J.H.G. Owen, D.R. Bowler, C.M. Goringe, P.T. Hayden, K. Miki, D.G. Pettifor, G.A.D. Briggs, J. Vac. Sci. Technol. A 16 (1998) 1938.
[29] I. Goldfarb, G.A.D. Briggs, J. Cryst. Growth 198–199 (1999) 1032.
[30] I. Goldfarb, G.A.D. Briggs, Surf. Sci. 433–435 (1999) 449.